

Possible astrophysical observables of quantum gravity effects near black holes

Ue-Li Pen^{1★} and Avery E. Broderick²

¹Canadian Institute for Theoretical Astrophysics, University of Toronto, M5S 3H8 Ontario, Canada, and Canadian Institute for Advanced Research CIFAR Program in Gravitation and Cosmology, M5G 1Z8 Ontario, Canada

²Perimeter Institute, Waterloo, N2L 6B9 Ontario, Canada

Accepted 2014 September 15. Received 2014 August 21; in original form 2014 January 10

ABSTRACT

Recent implications of results from quantum information theory applied to black holes have led to the confusing conclusions that require either abandoning the equivalence principle (e.g. the firewall picture), or locality, or even more unpalatable options. The recent discovery of a pulsar orbiting a black hole opens up new possibilities for tests of theories of gravity. We examine possible observational effects of semiclassical quantum gravity in the vicinity of black holes, as probed by pulsars and event horizon telescope imaging of flares. In some cases, pulsar radiation may be observable at wavelengths only two orders of magnitude shorter than the Hawking radiation, so precision interferometry of lensed pulsar images may shed light on the quantum gravitational processes and interaction of Hawking radiation with the space–time near the black hole. This paper discusses the impact on the pulsar radiation interference pattern, which is observable through the modulation index in the foreseeable future, and discusses a possible classical limit of non-locality.

Key words: black hole physics – gravitation – gravitational lensing: weak – pulsars: general.

1 INTRODUCTION

The recent discovery of PSR J1745–2900 (Eatough et al. 2013; Rea et al. 2013; Shannon & Johnston 2013) orbiting the galactic centre black hole (BH) opens up new possibilities for precision tests of gravity. It allows us to investigate possible outcomes as its orbit is mapped and possible quantum deviations from standard Einstein gravity.

It has proven challenging to find experimental consequences of quantum gravitational effects. At the same time, precision experimental probes of classical general relativity have a dearth of alternate theories to compare with.

In this paper, we explore possible semiclassical consequences of pulsar–BH binaries and flares in the galactic centre BH accretion flow. This is meant to stimulate concrete discussions of quantum mechanics applied to gravitational systems in scenarios that may be testable in the foreseeable future.

2 MOTIVATION

The quantum mechanical nature of BHs has provided a fruitful test bed for thought experiments and discussions. Hawking’s calculation

led to the possibility of BH radiation and evaporation. The radiation appears thermal, and appears not to depend on the interior of the BH, or its formation history. This leads to the well-known information loss problem (Hawking 1976).

Historically, the resolution of the problem included violation of unitarity (i.e. causality), or the possibility of remnants. String theory is a constructive example which is unitary and contains the same BH entropy and evaporation, and no remnants. In this context, the resolution of the paradox has to lie in the purity of Hawking radiation versus the breakdown of the equivalence principle near the horizon. As discussed in Almheiri et al. (2013, hereafter **AMPS**), a modification of Hawking radiation purity requires macroscopic changes in space–time of order unity outside the Schwarzschild radius (see also Mathur 2009 for a complementary view). Different groups arrive at opposite aesthetic conclusions from this line of reasoning: the firewall (**AMPS**) picture maintains radiation purity, and instead sacrifices the equivalence principle for infalling observers, who burn up at the horizon.

AMPS conclude that alternatives to firewalls predict macroscopic non-locality outside of the horizon. Despite various theoretical explorations, the nature of this non-locality remains poorly understood quantitatively (Giddings 2012; Devin 2014). Thus, in this paper we examine potential observable consequences that naturally arise in this non-local picture. Specifically, in this *paper* we investigate such non-local scenarios to explore possible consequences for quantum

* E-mail: pen@cita.utoronto.ca

measurement using pulsar radiation, using wavelengths comparable in energy to the Hawking radiation. This opens up the possibility of testing physics using real experiments instead of aesthetic considerations.

Pulsars are highly compact, very bright light sources and exquisite clocks, enabling precision measurements of space–time. A pulsar orbiting a BH provides a scenario which accentuates potential experimental outcomes. Very recently, the first candidate has been discovered (Eatough et al. 2013; Rea et al. 2013; Shannon & Johnston 2013), likely orbiting the Galactic centre BH. While the orbital parameters are not known to the author, there is a possibility that its orbit in projection passes close behind the BH, such that a gravitationally lensed image becomes visible. Depending on orbital parameters, such a conjunction could take decades to occur during which time more pulsar–BH binaries may be discovered. In addition to the Galactic Centre supermassive BH–pulsar binary, 10 double neutron star systems are known, and discovery of a pulsar–stellar mass BH binary appears likely (Belczynski, Kalogera & Bulik 2002). For purposes of this discussion, slow and fast pulsars are both suitable, with slow pulsars dominating the predicted populations. This is one of the goals of the planned Square Kilometre Array.¹

3 STRONG GRAVITATIONAL LENSING

We begin by considering the appearance of the image of a pulsar orbiting a BH. As a pulsar passes behind a BH, multiple images of the pulsar appear. In the weak field limit, one sees two images. This phenomenon is called ‘strong lensing’. In the strong field regime, an infinite number of exponentially fainter images appear (Rafikov & Lai 2006; Boyle & Russo 2011). In this section, we will confine our discussion to the two images under ‘weak field’ strong gravitational lensing.

We will consider the regime where the pulsar is many Schwarzschild radii behind the BH, and the weak field limit applies, with only small perturbations. The pulsar radiation is lensed by the BH’s gravitational field, which is well described by geometric optics. We first review the geometric optics, and then estimate the interference pattern of this double-slit experiment.

Generally, the brighter image is further away from the BH, and less affected by post-Einsteinian effects. This two-image scenario is much like a quantum double-slit experiment. For stellar mass BHs, the wavelength of the photons is not drastically different from that of the thermally emitted Hawking radiation photons, and is expected to probe the low-energy limit.

A background source always has two images: one inside the Einstein radius, which we call the interior image, and one outside the Einstein radius, the exterior image. The Einstein radius is defined in Schneider, Ehlers & Falco (1992)

$$\theta_E = \frac{\sqrt{r_s D_{ds}}}{D_d}, \quad (1)$$

where the Schwarzschild radius $r_s = 2GM/c^2$, D_{ds} is the distance from the BH to the pulsar and D_d is the distance to us. We are considering the limit where $r_s \ll D_{ds} \ll D_d$. From here onward, we will use units where the speed of light $c = 1$. The apparent image positions for a source at angular separation β are at

$$\theta_{\pm} = \frac{1}{2} \left(\beta \pm \sqrt{\beta^2 + 4\theta_E^2} \right), \quad (2)$$

with magnifications

$$\mu_{\pm} = \frac{u^2 + 2}{2u\sqrt{u^2 + 4}} \pm \frac{1}{2}, \quad (3)$$

where $u = \beta/\theta_E$ (Mao 1992). For large separations, the interior image gets faint as $1/u^4$, while the exterior image goes to its unlensed brightness. The time delay between the two images is

$$\Delta t = r_s \left[\frac{1}{2} u \sqrt{u^2 + 4} + \ln \frac{\sqrt{u^2 + 4} + u}{\sqrt{u^2 + 4} - u} \right]. \quad (4)$$

We now consider potential non-local corrections to this standard picture. In Schwarzschild coordinates, the metric is

$$ds^2 = -[1 - \psi(r)]dt^2 + [1 - \psi(r)]^{-1}dr^2 + r^2d\Omega, \quad (5)$$

with $\psi(r) = r_s/r$. For a light source many r_s away, the lensing equation depends on the projected potential $\varphi(\theta) = 2 \frac{D_{ds}}{D_d^2} \int \psi(\sqrt{(\theta D_d)^2 + z^2}) dz$. We consider a general multipole expansion of the potential, which in projection becomes

$$\varphi(\theta, \phi) = \theta_E^2 \ln(\theta/\theta_E) + \theta_E^2 \sum_m \frac{a_m \theta_s^m \cos[m(\phi - \phi_m)]}{\theta^m}, \quad (6)$$

with the apparent Schwarzschild radius $\theta_s = r_s/D_d$. We define the ratio $b \equiv \theta_E/\theta_s$, which is the impact parameter of the lensed image in units of Schwarzschild radii. The generic orbit has $b \gg 1$, and our data probe $\theta \sim \theta_E$. In Einstein gravity, $a_m = 0$ for $m \neq 2$, with the latter inheriting contributions from angular momentum. In a non-local quantum gravity scenario, at these large radii, the low- m harmonics dominate. Since the deviations to the space–time are of order unity near the horizon, one expects a_m to be order unity, and by isotropy the ϕ_m are uniformly distributed. In a firewall picture, one might expect all coefficients $a_m = 0$.

The lowest order perturbation is a dipole, $m = 1$. This is analogous to a displacement of the BH position by a Schwarzschild radius. This results in a variation of time delay

$$\delta\Delta t = \alpha \frac{r_s}{b} \left(\frac{\lambda}{r_s} \right)^{\gamma}, \quad (7)$$

for order unity proportionality constants α and γ . In Einstein gravity, $\alpha = 0$.

One might ask if $m = 0$ perturbations could result from non-local quantum gravity. The authors are agnostic on this question, which would correspond to an order unity fluctuation at all radii. It seems conceptually a larger step to give up the classical limit at arbitrarily large radii, but human knowledge in quantum gravity is certainly incomplete. Interference patterns would never be observed for expected astrophysical parameters in such a case.

In a non-local scenario, the delayed pulse will appear broadened: its pulse profile will appear wider, convolved by the distribution of delays from the different multipole perturbations. While the actual separation of images may be challenging to resolve in angle, the delays are readily observable. As in interstellar plasma lensing, the multiple images interfere constructively and destructively when observed in a single-dish telescope (Pen & King 2012).

Typical pulsars have the most sensitive detections at \sim GHz. In a classical BH, this results in a very precise measurement of delay and Doppler shift: with a 1 GHz bandwidth, delays are measurable to a nanosecond. The characteristic delay Δt for a solar mass BH is several microseconds, and expected fluctuations smaller by b . For a given set of orbital parameters, the fringe pattern is fully determined, and can be tracked. After shifting the self-interference pattern by the geometric delay, one is sensitive to the stochastic

¹www.skatelescope.org

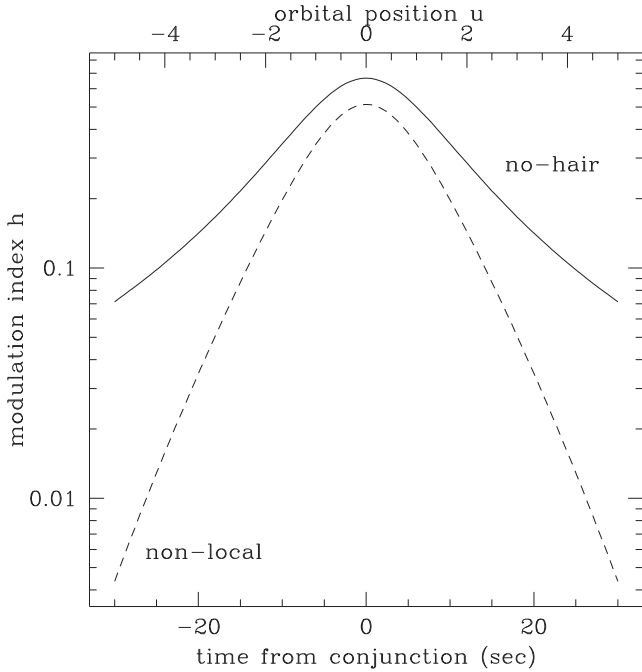


Figure 1. Pulsar modulation index. The aesthetic choice of ‘no-hair’ is thought to result in a firewall, with classical modulation index shown by the solid line. The alternative choice embracing an equivalence/complementarity principle, and thus rejecting the firewall, could lead to the dashed line, where the modulation index is reduced due to exterior quantum effects.

quantum fluctuations in time delay (equation 7), which induce phase differences of order unity for $b \lesssim 1000$.

To estimate the observational signature, we consider a pulsar orbiting a $2 M_{\odot}$ BH, at $4 \times 10^4 r_s$. This is intended to be just above the upper mass limit of neutron stars, above which they are expected to turn into BHs. The orbital period is 2 h, and gravitational radiation decay time $\sim 10^7$ yr, comparable to the lifetime of a slow pulsar (the most common type; Pfahl, Podsiadlowski & Rappaport 2005). We use an inclination of a quarter degree, which leads to conjunction at one Einstein radius. The intensity modulation index $h^2 \equiv \langle \delta I^2 / I^2 \rangle$ (Lorimer & Kramer 2012) resulting from the interference pattern depends on the orbital phase, and is shown in Fig. 1. We model the phase change in equation (7) as a Gaussian random field, which changes every dynamical time. For illustration convenience, we took the prefactor $\alpha \sim 10$, $\gamma = 1$. In a future data set, one could fit for α , γ from the data. The first principles computation of the parameters is beyond the scope of this paper, which we leave as a future exercise. The modulation index results from the interference of the two images in equation (3)

$$h = 2 \frac{\sqrt{\mu_+ \mu_-}}{\mu_+ + \mu_-}. \quad (8)$$

We note that the modulation index does not depend on wavelength, as long as the wavelength is shorter than the path difference in equation (4). The flux fluctuates with frequency and time with a fractional amplitude described by the modulation index. The modulation rate is uniquely predicted in Einstein gravity, and can be compared to data at precisions related to the wavelength divided by the signal-to-noise of the measurement. Two types of deviations are tested: the position and delays could differ classically. If the fluxes of individual images are independently measured, e.g.

through scintellometry (Pen & Levin 2014), the modulation index is an additional model-independent test.

We used an observing wavelength of $\lambda = 20$ m, the low end of the LOFAR² telescope. In a non-local, non-firewall scenario, the modulation index is decreased by $\exp(-\lambda^2/2\delta t^2)$, as is apparent in this picture. The fractional effect is the smallest at superior conjunction, when the inner image is the furthest from the BH, and thus has the least quantum effects.

PSR J1745–2900 is currently about 1 million Schwarzschild radii away from the galactic centre BH, in projection. If its orbit is inclined within 0.1 per cent to the line of sight, gravitational lensing effects become order unity. In this particular system, plasma scattering decoheres the radiation by $\delta t_s \sim (\text{GHz}/\nu)^4$ s, and at frequencies of \sim THz, the scattering becomes negligible. It is not known how bright the pulsar is at THz frequencies. The ALMA³ telescope might detect the pulsar at these frequencies. The gravitationally lensed images will form an interference pattern if the emission size is less than $\sim \lambda \theta_E / \theta_s$, or about 1 m. Some pulsar emission, for example Crab giant pulses, are thought to come from regions sufficiently compact to scintillate. Current plasma lensing limits the emission size to be less than about a kilometre (Johnson, Gwinn & Demorest 2012; Pen et al. 2014). There is about a 0.1 per cent chance that this pulsar will have a favourable orientation to test quantum gravity. It would seem prudent to search for more BH pulsar candidates, encouraged by the discovery of this first one. In this example, the observable wavelength is 12 orders of magnitude shorter than the Schwarzschild radius, and effects are only present for $\gamma \sim 0$.

One might worry that plasma effects confuse quantum gravity. While the presence of plasma lensing could certainly overwhelm gravitational lensing in some systems, this should not lead to a misidentification. The BH signal is periodic in the orbit, while line-of-sight effects should be random. Plasma local to the system could also lens the radiation. The plasma refractive index depends on wavelength squared, and maintains coherence of radiation. Holography of propagation effects can be used to remove plasma distortions, or even be used constructively to resolve the gravitationally lensed images, enabling a direct measure of phase coherence (Pen & Levin 2014; Pen et al. 2014).

To summarize the observational test of pulsar lensing phase coherence, AMPS showed that alternatives to a firewall may result in a non-local picture. This then predicts that the interior image undergoes substantial phase changes, of the order of r_s/b . For wavelengths longer than that, the interference pattern should be observable, and for shorter wavelengths, it should weaken and disappear. In the course of the orbit, this will change, with the fractional non-local impact minimized during conjunction (assuming conjunction is outside the Einstein radius). Finite emission size could also lead to an absence of an interference pattern. This has a different dependence on lensing geometry, so again seems unlikely to mimic the signal.

4 ACCRETION FLOW FLARES

The Event Horizon Telescope (EHT)⁴ could image radiation emitted by the plasma near the horizon of the galactic centre BH. This flow is known to be unsteady, with flares and other phenomena, which are strongly lensed (Broderick & Loeb 2005). As for the pulsar case, the accretion flow and flare are classical objects, and expected to follow

²<http://www.lofar.org/>

³www.almaobservatory.org

⁴<http://www.eventhorizontelescope.org/>

the classical dynamics. The low-energy photons emitted from the flare are low-energy probes, and subject to interaction in a non-local picture. Here, the effects would be large. The interior lensed image would appear extended, i.e. fuzzy. Normally, this fainter image, the one closer to the BH, is smaller due to conservation of surface brightness. The opposite could happen in a non-local picture: any lensed image would maintain a constant minimum size $\theta_s \sim 20\mu$ arcsec due to the fuzziness. For a flare smaller than this size, deviations could be observable. The open question is the energy dependence of such fluctuations.

EHT experiments are unlikely to show interference between lensed images, since accretion disc emission is generally extended. Here, the test would rely on localized flares, where multiple strongly lensed images would be visible, and time profiles are observables.

5 DISCUSSION

The lensing framework gives a simplified picture to discuss Hawking radiation entanglement. Instead of the typical $\exp(10^{-80})$ microstates, we can focus on the low-order multipoles, reducing the variables to a_1, θ_1 . To clarify the situation further, we consider a further restricted subspace: $\phi_1 = 0$, with the axis chosen such that the classical interior lensed image is at $\phi = 0$. We will further restrict $a_1 \in \{-1, 1\}$, i.e. a two-state system $|+\rangle, |-\rangle$, and consider a pure state BH. Any incoming photon state becomes entangled with the perturbed lensing eigenstates: $|i\rangle = \xi|+\rangle + \eta|-\rangle$, where $|\xi|^2 + |\eta|^2 = 1$. It may be perturbed outwards (\uparrow) or inwards (\downarrow), resulting in a different phase delay as discussed above. An ensemble of photons, as expected from pulsars or flares, is projected one photon at a time. This has some analogies to Stern–Gerlach space quantization, with the distinction that here the deflection field is quantum mechanical, perhaps like SQUID quantum superposition experiments (Friedman et al. 2000). The photon becomes effectively entangled with the BH.

In any matter flow, for example an orbiting neutron star or accretion flow, one needs to compare the rate at which particles exchange energy with each other, compared to the differential energy shift from the entanglement. For a star the outcome is clear: its large internal degrees of freedom lead to decoherence, and they probe an average space–time, which is Schwarzschild. For the flare under consideration, the fact that a lensing measurement requires the flare to be small compared to its orbital radius requires its self-interaction to be larger than the differential tidal effect, and the flare is also treated classically.

This analysis combines uncertain speculation from opposite opinion camps on the nature of BH evaporation. We caution that the scenario is by no means inevitable. A full discussion of the practicality of weak space–time measurements will be presented in a forthcoming publication.

6 SUMMARY

We have explored semiclassical quantum effects of BHs. A pulsar–BH binary provides a concrete setup where such effects might become observable. This proposed experiment distinguishes between classical measurements in a Kerr–Schwarzschild space–time, such as a star orbiting a BH, and quantum measurements, such as the interference of two light paths bent by the gravitational field of the BH. The interference pattern could be changed by the quantum nature

of the BH if the resolution of the Hawking paradox lies in the non-purity of Hawking radiation. The outcome is speculative in nature, and is hoped to stimulate further investigation of non-Einsteinian outcomes of strong lensing experiments. We have argued that the recent pulsar–BH system, and likely more future discoveries, allows a precise test of space–time using double-slit interferometry and coherence of space–time. This may allow us to probe new aspects of quantum gravity. The modulation index in classical physics is uniquely determined by the brightness of image (possibly measurable using scintillometry), while quantum mechanics could modify that relation. At least, until the ideal pulsar–BH system is discovered, it provides a new sandbox to test ideas, to answer questions about complementarity and the interaction of Hawking radiation with space–time.

ACKNOWLEDGEMENTS

We are grateful to Samir Mathur, Don Page, Jason Gallicchio, Aephraim Steinberg, Daniel James and Aggie Branczyk for stimulating discussions. UP thanks the Tsinghua University for Advanced Studies where this work was completed. The work was supported by NSERC and CIFAR. AEB receives financial support from the Perimeter Institute for Theoretical Physics and the Natural Sciences and Engineering Research Council of Canada through a Discovery Grant. Research at Perimeter Institute is supported by the Government of Canada through Industry Canada and by the Province of Ontario through the Ministry of Research and Innovation.

REFERENCES

- Almheiri A., Marolf D., Polchinski J., Sully J., 2013, *J. High Energy Phys.*, 2013, 62 (AMPS)
- Belczynski K., Kalogera V., Bulik T., 2002, *ApJ*, 572, 407
- Boyle L., Russo M., 2011, preprint ([arXiv:1110.2789](https://arxiv.org/abs/1110.2789))
- Broderick A. E., Loeb A., 2005, *MNRAS*, 363, 353
- Devin M., 2014, *Galaxies*, 2, 189
- Eatough R. P. et al., 2013, *Nature*, 501, 391
- Friedman J. R., Patel V., Chen W., Tolpygo S. K., Lukens J. E., 2000, *Nature*, 406, 43
- Giddings S. B., 2012, *Phys. Rev. D*, 85, 124063
- Hawking S. W., 1976, *Phys. Rev. D*, 14, 2460
- Johnson M. D., Gwinn C. R., Demorest P., 2012, *ApJ*, 758, 8
- Lorimer D. R., Kramer M., 2012, *Handbook of Pulsar Astronomy*. Cambridge Univ. Press, Cambridge
- Mao S., 1992, *ApJ*, 389, L41
- Mathur S. D., 2009, *Class. Quantum Gravity*, 26, 224001
- Pen U.-L., King L., 2012, *MNRAS*, 421, L132
- Pen U.-L., Levin Y., 2014, *MNRAS*, 442, 3338
- Pen U.-L., Macquart J.-P., Deller A. T., Brisken W., 2014, *MNRAS*, 440, L36
- Pfahl E., Podsiadlowski P., Rappaport S., 2005, *ApJ*, 628, 343
- Rafikov R. R., Lai D., 2006, *Phys. Rev. D*, 73, 063003
- Rea N. et al., 2013, *ApJ*, 775, L34
- Schneider P., Ehlers J., Falco E. E., 1992, *Gravitational Lenses*. Springer-Verlag, Berlin
- Shannon R. M., Johnston S., 2013, *MNRAS*, 435, L29

This paper has been typeset from a $\text{\TeX}/\text{\LaTeX}$ file prepared by the author.